

# Data reduction and analysis of Solar Dopplergrams

A. Cacciani<sup>1</sup>, P. Rapex<sup>1</sup>, B. Subrizi<sup>1</sup>  
and V. Di Martino<sup>2,\*</sup>

<sup>1</sup> Dep. of Physics, Univ. of Roma La Sapienza, P.le A.Moro 2, I-00185, Roma, ITALY

<sup>2</sup> CASPUR, via dei Tizii 6b, I-00185 Roma

**Abstract.** Helioseismology studies requires the acquisition and analysis of sequence of line-of-sight velocity fields of the solar atmosphere. To obtain such velocity maps of the full solar disk a doppler shift analysis of the emitted photons is performed. Such velocity fields are commonly indicated as dopplergram. It is necessary to correctly correlate each pixel position corresponding to the same piece of the solar atmosphere evolving in time. Such time series analysis require a software procedure to aline acquired raw images that may be different in size and position. In this presentation we show how we perform such data reduction using ad hoc software, that in some cases require an human interaction for validation to prevent the lost of single images geometric characteristic. Almost all the images geometric characteristic are automatically identified by our registration code. Due to the optional human intervention we classify this software as a graphical interface for solar data post processing.

**Key words.** Image processing – Sun: helioseismologycosmology

## 1. Description of the Instruments

The Magneto Optical Filter is a compact instrument to acquire dopplergram of the Na D2 line and of the K line (3) (4), (5), (6). A photo of the instrument is provided in fig: 1. It filter properties are obtained using an active vapor media where polarization of incident photons are changed only for photons in a narrow bandwidth, see schema in fig: 2. In the previous instrument the data were collected by a 8 bit ccd

at TV frequency, each frame were accumulated on two different buffer and odd and even frames were switched to red and blue doppler shift wing. In this arrangement the same camera and the same optical path was used to acquire the two images. In the new instruments the red and blue images are acquired and accumulated on 2 ccd at 12 bit directly on the PC memory. In the second case the ccd pixel response and geometric image distortion may add a spurious signal and accurate image registering is necessary just to obtain the velocity field im-

---

\* Contact email address: vincenzo@caspur.it



**Fig. 1.** A photo of the compact MOF instrument, on an equatorial mount.

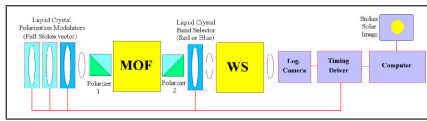


**Fig. 2.** Functional schema of the MOF instrument and the wing selector, this schema require that the liquid crystal polarizer is synchronized with single frame ccd acquisition, the cell may contain Na or K vapors

ages. Description of the new instruments is given in (1).

## 2. MOF dopplergram and magnetogram

In this section we give a sample of raw images acquired by the instrument, this have been the starting images for the post processing procedure. There are two kind of images dopplergram as in fig. 3, and magnetogram fig. 4. The two images may be recombined to avoid contamination of dopplergram due to intense magnetic field at the solar surface, as in fig. 5. The maximum value of the doppler signal may be seen taking the difference of two images at about 2,5 minutes of distance, as is shown in fig. 7, in this way also the effect of the solar rotation is subtracted as well as the relative sun earth velocity and earth rotation radial velocity that change the position of the 0 value of the solar rotation axis. All the images shown here have been already

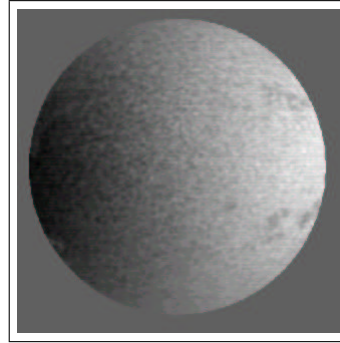


**Fig. 3.** Doppler data for the Na D1,D2 lines, in the right side of the image there is the spurious effects due to sun spots and relative high magnetic fields.

centered by the procedure below described, the real raw data is of about 760x512 pixel as shown in fig. 6. Unfortunately due to instrument guiding and different atmosphere distortion the images are subject to be shifted inside the ccd active area during the 24 hour acquisition period. This is why we needed the image registration below described. Another apparent movement that must be compensated is the rotation of the solar disk on his center of view due to the Celostat arrangement. Using equatorial mounted instrument this registration is unnecessary.

## 3. Solar rotation axis inclination detection

To detect automatically the relative position of the solar rotation axis we develop a fitting procedure using contour lines of the velocity images. The human eye is capable to individuate such axis looking at images like in fig. 8 where the smaller details have been removed averaging near by pixel values like in a rebinning procedure. Numerical procedure have to use several contour lines to fit this inclination angle value, see fig. 9

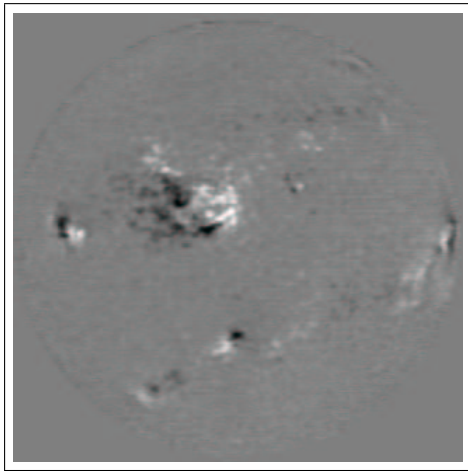


**Fig. 4.** Example of a longitudinal magnetic field image obtained using 4 different polarization selected frames of a MOF

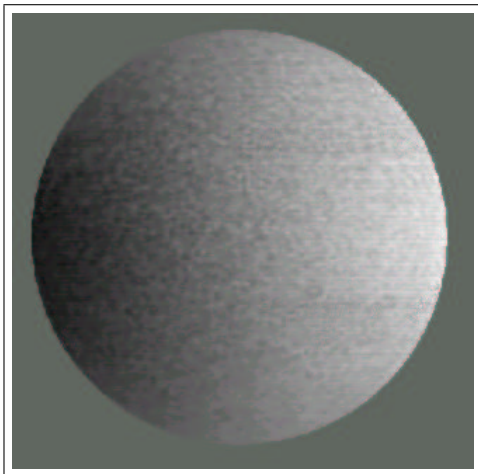


**Fig. 5.** Example of image restored signal when the magnetic contamination on the data is numerically compensated

#### 4. Solar image center, ellipsoid fit

To analyze the power spectrum of the solar resonant sound waves oscillation it is necessary to observe the surface as long as possible. Due to experimental setup and atmospheric perturbation the acquired images are not centered in the same position, giving a random shift in the solar disk cen-

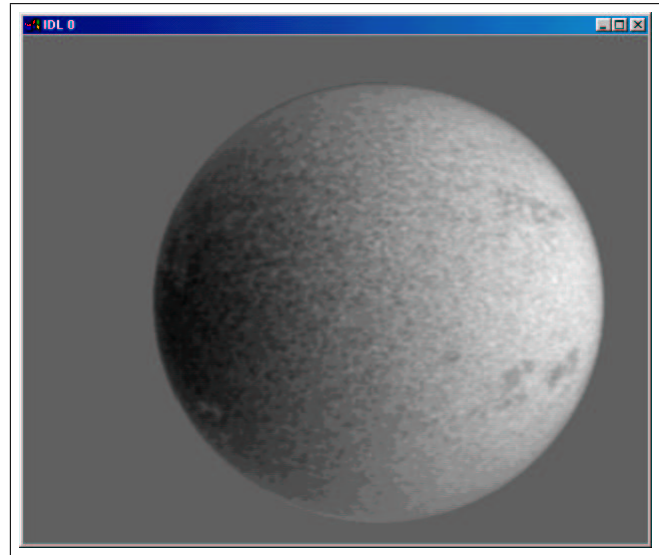


**Fig. 6.** Example of doppler image as acquired by the old ccd at TV resolution, image position translate during the day, due to experimental setup and atmospheric condition

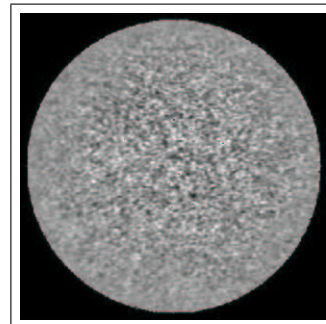


**Fig. 7.** Example of doppler image with solar rotation detrended and maximum velocity field signal, obtained taking the difference of two dopplergram 2-3 minutes apart.

ter. Atmospheric condition and sun height respect to horizon as well as relative humidity of the atmosphere during the day night cycle at the Baia Terranova station in Antarctica produce changes in the dimension and distortion of the solar disk image. To track such changes we fit the solar limb

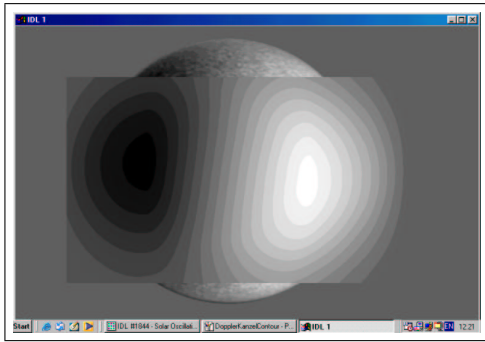


**Fig. 8.** solar Rotation axis relative inclination detection, human eye take advantage of smoothed image to eliminate solar oscillation to evidence the linear signal due to sun rotation.

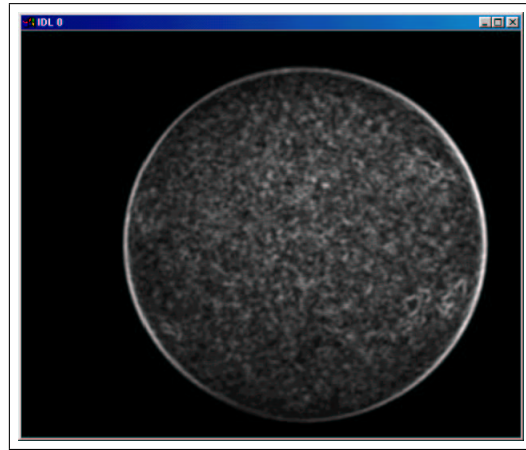


**Fig. 10.** Edge detection of the solar limb enhanced by a Sob-el filter.

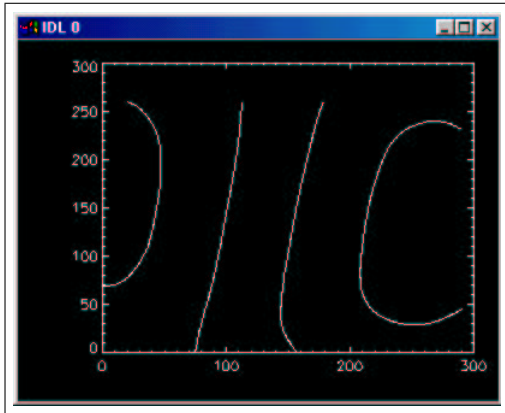


**Fig. 9.** Contour lines to be fitted by a line for automatic axis rotation inclination detection.

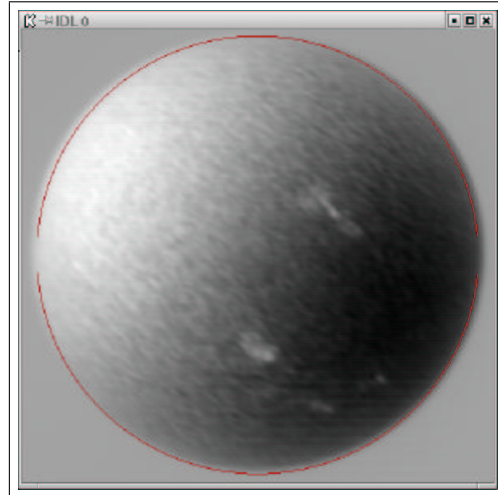


**Fig. 11.** Ellipse fitting of the solar limb region to take account of solar disk distortion due to atmospheric interference.

with an ellipse. Graphical example of such fitting procedure is given in fig. 11, 13, 10, 12. All of this procedures have an overall precision that depends by the quality of the starting image and is at the best in the order of 0.5 pixel for procedure shown in fig. 11 and 0.2 pixel for procedure shown in fig. 13 based on the intermediate step shown in fig. 10, 12.

## 5. Solar oscillation power spectrum

In this last session we compare the power spectrum diagrams plotted versus  $l$  mode number value, where  $l$  is the secondary principal number of the spherical harmonic mode decomposition, and the frequency  $\nu$ . Different values of the  $m$  are summed up for each  $l$  value. In fig. 15 we show the result obtained using the Software package

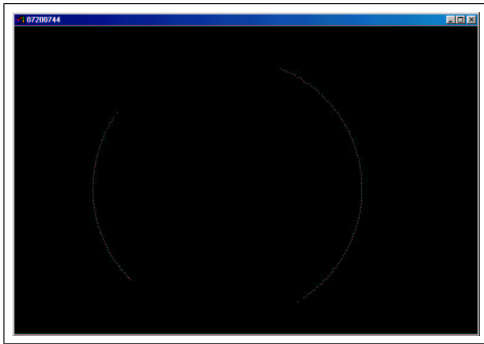


**Fig. 12.** Starting point for another ellipse fitting procedure on a set of points on the solar limb.

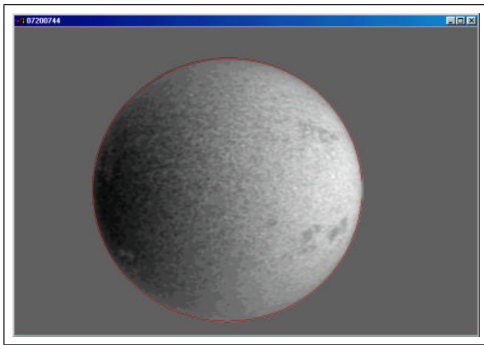


**Fig. 13.** Ellipse fitting of the solar limb region at 0.2 pixel precision for the estimated center of the sun disk.

IRAF developed by several programmers at NOAO for the GONG project. In fig. 16 we show the result for the power spectrum for a shorter period obtained with our in home IDL procedure.

## 6. Conclusions

In this paper we present a set of software procedure for image registration and restoration. All of them developed in the IDL graphical environment permit to visualize the obtained results. This graphical procedure are used to run post processing analysis of solar dopplergram at the University of Rome at the department of Physics and at CASPUR. A new experi-

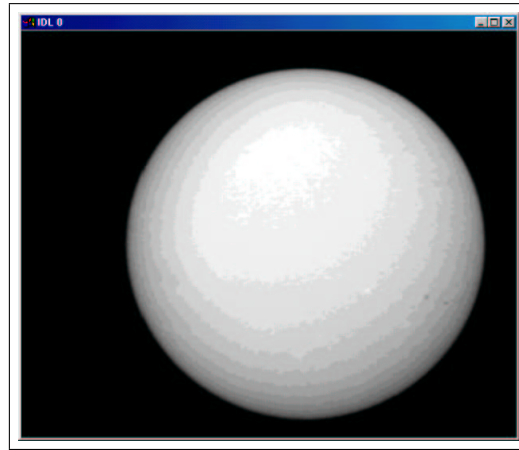


**Fig. 14.** Intensity image for precise sun disk centering, if the image was symmetric a 0.01 pixel resolution could be reached for images acquired in good atmospheric condition.

ment as been set up and is currently acquiring data at the Scott Amundsen base at South Pole. For this experiment there will be the necessity to run flat field correction for non linear response of CCD pixels. In this new experiment 4 different images will be stored every 10 seconds producing an overall solar image data dimension of about 1.5 Terabyte, we will apply such registration procedure to this new dopplergram data set.

## References

- Cacciani, A., Jefferies, S. M., Finsterle W., Rapex, P., Knox, A., Giebink, C., and, Di Martino, V.: 2002, A new instrument for sounding the solar atmosphere, Big Bear 11/2002 SOHO 12/GONG+ 2002 meeting
- Ando, H. and Osaki, Y.: 1977, "The Influence of the Chromosphere and Corona on the Solar Atmospheric Oscillations", Publ. Astr. Soc. Japan, 29, 221
- Cacciani, A. and Fofi, M.: 1978, "The Magneto-Optical Filter. II. Velocity Field Measurements", Solar Phys., 59, 179

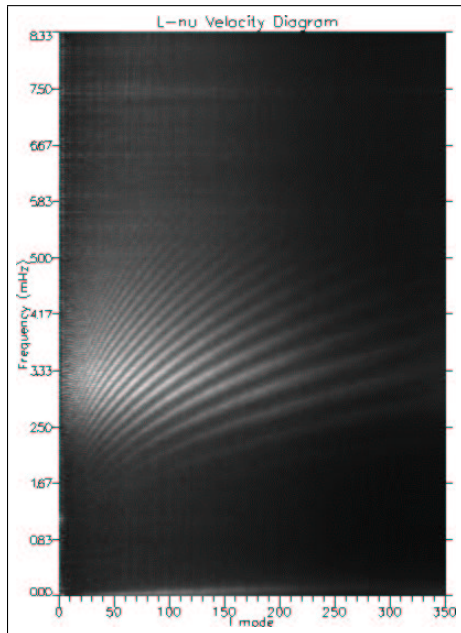


**Fig. 15.** Power spectrum plotted for different value of  $l$  and different frequencies, obtained using the IRAF/GRASP SW package

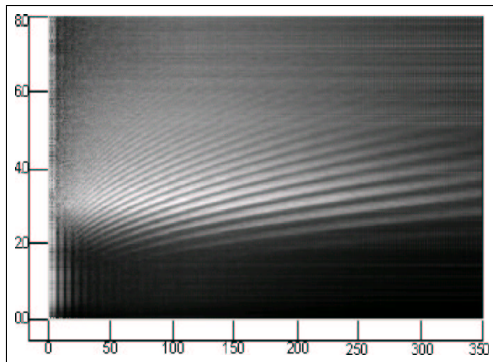


**Fig. 16.** Power spectrum for a 6 hour image acquisition run, obtained using in house IDL subroutine

Cacciani, A., Rhodes, E. J. Jr., Smith, E., Tomczyk, S., and Ulrich, R. K.: 1988, "Acquisition and Reduction Procedures for MOF Doppler Magnetograms", in *Seismology of the Sun and Sun-like Stars*, ed. E.J. Rolfe, ESA SP-286, 185

Cacciani, A., Rosati, P., Ricci, D., Egidi, A., Appourchaux, T., Marquedant, R. J., and Smith, E. J.: 1994, "Theoretical and Experimental Study of the Magneto-Optical Filter", JPL Report No. D11900

Cacciani, A.: 1996, private communication

Deubner, F. -L., Waldschik, Th., and Steffens, S.: 1996, "Dynamics of the Solar Atmosphere. VI. Resonant Oscillations of an Atmospheric Cavity: Observations", *Astron. Astrophys.*, 307, 936

Duvall, T. L. Jr., Jefferies, S. M., Harvey, J. W., and Pomerantz M. A.: 1993, "Time-Distance Helioseismology", *Nature*, 362, 430

Duvall, T. L. Jr., D'Silva, S., Jefferies, S. M., Harvey, J. W., and Schou, J.: 1996, "Downflows Under Sunspots Detected by Helioseismic Tomography", *Nature*, 379, 235

Fleck, B. and Deubner, F. -L.: 1989, "Dynamics of the Solar Atmosphere. II. Standing Waves in the Solar Chromosphere", *Astron. Astrophys.*, 224, 245

Grossman-Doerth, U.: 1994, "Height of formation of solar atmospheric spectral lines", *Astron. Astrophys.*, 285, 1012

Jefferies, S. M., Pfeiffer, R., Pomerantz, M. A., Schulman, L., and Ball, W.: 1989, "A Solar Tracking Platform for use at the South Pole", in *Astrophysics in Antarctica*, ed. D. J. Mullan, M. A. Pomerantz, and T. Stanev, AIP Conf. Proc. 198, New York, 222

Jefferies, S. M.: 1998, "High-Frequency Solar Oscillations", "New Eyes to See Inside the Sun and Stars. Pushing the Limits of Helio- and Asteroseismology with New Observations from Ground and from Space", ed. F. L. Deubner, IAU Symposium 185, 415

Linskey, J.: 1989, "Solar and Stellar Observations from the South Pole", in *Astrophysics in Antarctica*, ed. D. J. Mullan, M. A. Pomerantz, and T. Stanev, AIP Conf. Proc. 198, New York, 205